Biophysical Journal Volume 108 May 2015 2562–2572

Article

Annealed Random Copolymer Model of the B-Z Transition in DNA: Torsional Responses

Ah-Young Kwon,[1] Nam-Kyung Lee,[1,2,*] Seok-Cheol Hong,[3] Julien Fierling,[2] and Albert Johner[1,2]
[1]Department of Physics, Sejong University, Seoul, South Korea; [2]Institute Charles Sadron, Centre National de la Recherche Scientifique, Strasbourg, France; and [3]Department of Physics, Korea University, Seoul, South Korea

ABSTRACT Both in vivo and in vitro, specific sequences in double-stranded DNA can adopt the left-handed Z-form when underwound. Recently, the B-Z transition of DNA has been studied in detail in magnetic tweezers experiments by several groups. We present a theoretical description of this transition, based on an annealed random copolymer model. The transition of a switchable sequence is discussed as a function of energetic and geometric parameters of the B- and Z-forms, of the applied boundary conditions, and of the characteristics of the B-Z interface. We address a possible torsional softening upon the B-Z transition. The model can be also applied to other biofilaments with annealed torsional/flexural degrees of freedom.

INTRODUCTION

In nature, DNA is often subjected to torque and force, particularly during transcription. This prompted in vitro studies to examine the twist-extension curve (bell curve) (1,2) under various tensions with special emphasis on the picoNewton range. The prominent technique for these studies is single-molecule manipulation with magnetic tweezers, which can directly add extra turns to a stretched DNA. A number of DNA structures were detected and most of them were characterized by their pitch and elastic moduli. A rich behavior emerges when the standard B-form is underwound. At low tension, <1 pN, the torsional stress is relaxed by the formation of plectoneme while at higher tension the B-form unwinds and results in a left-handed helix with slightly higher pitch (the L-form) (3,4). For a random sequence, the critical torque for unwinding is ~ -10 pN nm under physiological conditions and its magnitude slightly decreases with increasing tension. "L-form" is a rather broad concept for all kinds of (predominantly) left-handed DNA. Generally, the structure of the L-form is not stabilized by hydrogen bonds, and thus, is rather labile. This results in a soft structure as manifested in the effective torsional modulus $C_L - k_B T l_L$ with the twist persistence length $l_L = 10-20$ nm, approximately one-order-of-magnitude smaller than for B-DNA ($l_B = 100$ nm) (5).

For specific sequences, like $(TG)_n$ or $(GC)_n$ dinucleotide repeats, it is possible to establish Watson-Crick pairs in the left-handed helix too (6,7). The resulting structure is called "Z-DNA", in reference to its (twisted) zig-zag geometry. Z-DNA is more stable than generic L-DNA from a random sequence (8). Several molecular mechanisms of the B-Z transition have been proposed (7,9).

From recent single-molecule experiments (10–12), a great deal of new information became available for Z-DNA. Lee et al. (10) investigated the B-Z transition induced by supercoiling at the single-molecule level and characterized the dynamics of the transition in short local $(GC)_n$ sequences with their newly-developed hybrid technique of single-molecule FRET and magnetic tweezers. From torque measurement, Oberstrass et al. (12) show the stability of Z-DNA over L-DNA manifested in a lower critical torque for the B-Z transition, ~ -2 pN nm in physiological conditions, as compared to the B-L transition at -10 pN nm. In such an assay, a core sequence that can form Z-DNA is embedded into a longer random sequence, in contrast to NMR experiments using short DNA oligomers where all basepairs can switch their structure together (13). The flanking sequences serve as handles in the single-molecule manipulation (5,10–12). The difference in the critical torque between Z-DNA and L-DNA (the difference in free energy per basepair) is large enough to switch the core sequence without even a partial switch of monomers in the handles.

Extensive studies of thermodynamic and structural properties of Z-DNA have been carried out over the last few decades mostly for plasmid DNA (6,14–17). More recently, detailed characteristics of Z-DNA and of the B-Z transition have been measured (5,7,10,18). Under physiological conditions and without specific proteins (chemicals) attached to it, Z-DNA is only stable under a sufficiently high negative torque. Electrostatics slightly disfavors the Z-form with respect to the B-form. On the other hand, the Z-form usually better accommodates the hydrophobic groups of the residues. At a sufficiently high salt concentration (in the molar range [3–4 M]), Z-DNA can become thermodynamically

Submitted August 11, 2014, and accepted for publication March 17, 2015.
*Correspondence: lee@sejong.ac.kr
Editor: Keir Neuman.

0006-3495/15/05/2562/11 $2.00
http://dx.doi.org/10.1016/j.bpj.2015.03.060

stable even in the absence of negative torque (15). Some proteins that predominantly bind to Z-DNA can locally nucleate the Z-form within a B-DNA (16). Examples of Z-DNA binding proteins are double-stranded RNA adenosine deaminase 1, vaccinia virus E3L, and DLM-1, among others. In a similar spirit, the Z-form can also be stabilized by some amines like spermine and spermidine (17). While proceeding, the transcription machinery imposes positive supercoiling ahead of the R-loop, which is released by topoisomerase, and negative supercoiling behind the R-loop, which can stabilize Z-DNA. It was proposed that Z-DNA recruits adenosine deaminase 1, which stabilizes Z-form, thereby enhancing its activity. On the other hand, Z-DNA can also stall the transcription machinery. Z-DNA is not just a curiosity, as the versatile roles of Z-DNA in many biological processes have been recently recognized (19).

Theoretically, thermodynamics of the B-Z transition has been addressed by Vologodskii and Frank-Kamenetskii (20) and Frank-Kamenetskii and Vologodskii (21) earlier. Later studies include statistical mechanics of Z-DNA (22) and excitation mechanism (9). To explain recent magnetic tweezers experiments (11,12,23,24) measuring the torque, some theoretical analyses using a partition function that accounts for Gaussian twist fluctuations are given (12). These existing theories rely on linear elasticity. In this article, we propose a theory for structural changes of DNA beyond linear elasticity. We apply this model to the B-Z transition where the DNA molecule under tension is represented as a chain of bonds with a prescribed twist-free energy. The most prominent difference between the Z-form and the B-form, both of which may be reasonably described by Gaussian bonds, is the preferred twist angle per bond, although other parameters like the torsional stiffness of the bond are also different. The debated B-Z interface needs specific modeling: the interface is known to be extended, and is unlikely to be governed by linear elasticity due to extruded (broken) basepairs.

Below, in Materials and Methods, we first describe the model and derive some useful relations that will be exploited in the Results section. We address the B-Z transition under several experimentally relevant boundary conditions. We also discuss the characteristics of the B-Z interface. Our study implies that the observed torsional softening upon the B-Z transition might in part come from the soft B-Z junction. Discussion and Conclusions summarizes our findings and discusses the main limitations of the model.

MATERIALS AND METHODS

We consider a DNA molecule that is subjected to a tension of several picoNewtons and hence stretched. The main geometrical parameter is the twist angle ψ, whose statistics is defined at any basepair of index n ranging from 0 to N (Fig. 1). The reference state with $\psi(n) = 0$ for any n corresponds to two parallel unwound strands. For any basepair, we need to additionally specify whether it is in the B-state or in the Z-state. The twist and state-propagation along the molecule is described as a Markovian process. The torsional statistics of the DNA polymer is reflected by the bond operators. The action of the bond operator is defined through the kernel $\mathcal{D}$, giving the (normalized) probability distribution of the twist-angle increment in the last bond. For a homopolymer chain (say, all in B-form), the partition function upon chain extension (from length n to length $n + 1$) reads

$$Z_{n+1}(\psi) = \int \mathrm{d}\delta\psi \mathcal{D}(\delta\psi) Z_n(\psi - \delta\psi).$$

Below we use Fourier-transformed quantities with q as the momentum conjugated to the twist angle ψ. The recursion relation then simplifies to $Z_{n+1}(q) = \mathcal{D}(q)Z_n(q)$. For simplicity, we work out the model for the most familiar case of linear (Gaussian) elasticity considered in earlier work (12), but we stay with the general formulation. While linear elasticity approximately applies for the B- and Z-forms, which are stabilized by hydrogen bonds, it is less satisfactory for describing open (unpaired) bubbles and the B/Z junction that comprises extruded basepairs. Indeed non-Gaussian behaviors are found for a flexible twisted homopolymer bubble with short-ranged excluded volume interactions (25) or connected loops with annealed topology (26) and even for a self-avoiding walk wrapping around a slender rod (27). Such systems present an extended twist regime where turns are taken at nearly constant torque and the partition function only decreases as a simple exponential of the linking number.

Within the regime of linear elasticity (Gaussian bond model), the B- and Z-states differ in their intrinsic twists, or preferred ψ increments, ψ_B and ψ_Z, respectively, between two consecutive basepairs. We may refine our description of the B-Z interface by introducing a specific preferred twist-angle increment between the adjacent B- and Z-basepairs, $\psi_{B\to Z}$ and a specific torsional elasticity, $l_{B\to Z}$. Their torsional moduli (l_B and l_Z) and their extensions (a_B and a_Z) along the DNA axis are also different (see Fig. 1). Switching one basepair from the B-state to the less favorable Z-state costs a free energy ϵ, the value of which depends on salt concentration, and there is a domain wall energy E accounting for the structural mismatch at the B-Z interface. All moduli and energies will be counted in thermal units (at room temperature).

Let the $\mathcal{Z}_i$ value be the partition functions under the constraint of having the end in state i. The $\mathcal{Z}_i$ values obey the following recursion equations:

$$\begin{aligned} \mathcal{Z}_B(n+1) &= \mathcal{D}_B \mathcal{Z}_B(n) e^{-\epsilon_B} + \mathcal{D}_{Z\to B} \mathcal{Z}_Z(n) e^{-\epsilon_B - E}, \\ \mathcal{Z}_Z(n+1) &= \mathcal{D}_Z \mathcal{Z}_Z(n) e^{-\epsilon_Z} + \mathcal{D}_{B\to Z} \mathcal{Z}_B(n) e^{-\epsilon_Z - E}. \end{aligned} \quad (1)$$

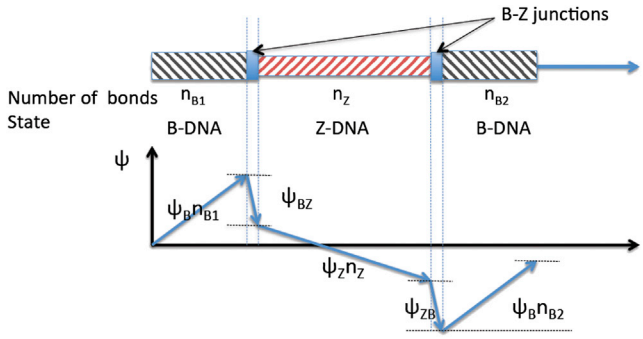

FIGURE 1 Scheme of the ψ along the DNA. The twist of the centerline is $\psi_B = 2\pi/10$ for B-state, $\psi_Z = -2\pi/12$ for Z-state. $\psi_J = \psi_{BZ} = \psi_{ZB}$ stands for the twist-angle change at the B-Z junction. To see this figure in color, go online.

The recursion formally starts out from $n = 0$ for an isolated basepair with $\mathcal{Z}_B(0) = e^{-\epsilon B}$ and $\mathcal{Z}_Z(0) = e^{-\epsilon Z}$. The index n measures the number of bonds in the chain under construction. To get rid of convolutions, the bond operator kernels $\mathcal{D}_i$ are expressed in reciprocal space in Eq. 1 with q as the variable conjugate to ψ. The Boltzmann weights in Eq. 1 complement the normalization of the bond operator: $\mathcal{D}_i(q = 0) = 1$. For operators of the elastic type, one simply has $\mathcal{D}_i = e^{iq\psi_i} e^{-\frac{a}{2l_i}q^2}$, whereas for a rigid interface entailing a prescribed shift ψ_i, we only have $\mathcal{D}_i = e^{iq\psi_i}$. To avoid unnecessary complication in notation, we introduced the single notation a for the length of a basepair regardless of the local state, which implies a renormalization of the moduli. In the same spirit, the ε_i and E are assumed to depend on the applied tension f in a straightforward way, like $\varepsilon_i = \varepsilon_{i,f=0} - fa_i$. Before proceeding, we may point out some natural rescalings, in order to reduce the number of explicit parameters. We are free to choose an origin for the free energy such that $\varepsilon_B = 0$, which corresponds to the rescaling $\mathcal{Z}_{B,Z} \to \mathcal{Z}_{B,Z}\exp(n\epsilon_B)$. Similarly we may choose the preferred twist of the B-state as reference under the rescaling $\mathcal{Z}_{B,Z} \to \mathcal{Z}_{B,Z}\exp(-iqn\psi_B)$. In the reciprocal space, the recursion relations in Eq. 1 are of the standard transfer matrix type. We may write down their formal solution as

$$\mathcal{Z}_i(n) \;=\; M_{i,j}\mathcal{Z}_j(0),$$

where $M_{i,j}$ explicitly depends on q through the bond operators,

$$\begin{aligned}
M_{B,B} &= -z_1^n \frac{e^{-\epsilon}\mathcal{D}_Z - z_1}{z_1 - z_2} + \text{permutation},\\
M_{B,Z} &= z_1^n \frac{e^{-E}\mathcal{D}_{Z\to B}}{z_1 - z_2} + \text{permutation},\\
M_{Z,B} &= z_1^n \frac{e^{-E-\epsilon}\mathcal{D}_{B\to Z}}{z_1 - z_2} + \text{permutation},\\
M_{Z,Z} &= -z_1^n \frac{\mathcal{D}_B - z_1}{z_1 - z_2} + \text{permutation},
\end{aligned} \tag{2}$$

where $z_{1,2}$ are the two roots of

$$z^2 - \left(\mathcal{D}_B + e^{-\epsilon}\mathcal{D}_Z\right)z - e^{-2E-\epsilon}\mathcal{D}_{Z\to B}\mathcal{D}_{B\to Z} + e^{-\epsilon}\mathcal{D}_B\mathcal{D}_Z \;=\; 0$$

and where $\varepsilon = \varepsilon_Z - \varepsilon_B$ is furnished with permutation of $1 \leftrightarrow 2$. The above results can also be obtained using a z-transform. (See the part after Eq. 11 where we solve a larger class of models using a z-transform.) The matrix $M_{i,j}$ can address various situations encountered in experiments (11,13). For example, if the core sequence is inserted between two stable (under the applied twist/torque) double-stranded B-DNA, the partition function is given by $\mathcal{Z}_{\text{fixed}} = M_{B,B}$, which we call the fixed-boundary case. If there is only one B-handle and the other end of the core sequence is free to switch, $\mathcal{Z}_{\text{mixed}} = M_{B,B} + M_{Z,B}$ applies, which we call the mixed-boundary case. The free-boundary condition refers to the case where both ends of the core sequence can freely switch and $\mathcal{Z}_{\text{free}} = (M_{B,B} + M_{Z,B}) + e^{-e}(M_{B,Z} + M_{Z,Z})$. These three cases are qualitatively different: For the fixed-boundary case, the B/Z transition involves an even number N_{DW} of domain walls (at least two), whereas for the mixed-boundary case the transition accommodates any number of domain walls (at least one). Under the free-boundary conditions, the Z-state can be accommodated without any domain wall. The partition functions in the reciprocal space as deduced from the expressions in Eq. 2 are useful for the case where the torque τ (rather than the twist angle ψ) is the control parameter (torque ensemble). Indeed, the partition function under imposed torque,

$$\mathcal{Z}_\tau \;=\; \int_{-\infty}^{+\infty} \mathrm{d}\psi \mathcal{Z}(\psi) e^{\tau\psi},$$

corresponds to the complex momentum $q = -i\tau$. A standard output is the equation of state of DNA, $\langle\psi\rangle = \frac{1}{\mathcal{Z}_\tau}\frac{\mathrm{d}\mathcal{Z}_\tau}{\mathrm{d}\tau}$. In classical thermodynamics, the Helmholtz free energy and Gibbs free energy are related by Legendre transform. If fluctuations are not vanishingly weak, as is the case here, the inverse Fourier transform of the partition function $\mathcal{Z}(q)$ is required to obtain (ψ). To be explicit, let us write down $z_{1,2}$:

$$\begin{aligned}
z_{1,2} &= \frac{1}{2}\left(\mathcal{D}_B + \mathcal{D}_Z e^{-\epsilon}\right) \pm \frac{1}{2}\sqrt{\Delta},\\
\Delta &= \left(\mathcal{D}_B - \mathcal{D}_Z e^{-\epsilon}\right)^2 + 4\mathcal{D}_{Z\to B}\mathcal{D}_{B\to Z}e^{-2E-\epsilon}.
\end{aligned} \tag{3}$$

In the following, $z_1(z_2)$ corresponds to the $\pm$ sign in Eq. 3. The explicit partition function with fixed-boundary conditions reads:

$$M_{B,B} \;=\; \frac{z_1^n}{2}\left(1 + \frac{\mathcal{D}_B - D_Z e^{-\epsilon}}{\sqrt{\Delta}}\right) + \frac{z_2^n}{2}\left(1 - \frac{\mathcal{D}_B - \mathcal{D}_Z e^{-\epsilon}}{\sqrt{\Delta}}\right). \tag{4}$$

For the mixed-boundary conditions the partition function is the sum $M_{B,B} + M_{Z,B}$, where

$$M_{Z,B} \;=\; \frac{e^{-E-\epsilon}\mathcal{D}_{B\to Z}}{\sqrt{\Delta}}\left(z_1^n - z_2^n\right). \tag{5}$$

As anticipated, for the fixed-boundary, the states with even powers of e^{-E}, including power 0, enter the partition function (Eq. 4), while for the mixed-boundary conditions the additional contribution shown in Eq. 5 introduces terms with odd powers of e^{-E}. Let us recall the simple Gaussian structure adopted for linear elasticity:

$$\begin{aligned}
\mathcal{D}_B &= e^{iq\psi_B}e^{-\frac{q^2 a}{2l_B}},\\
\mathcal{D}_{B\to Z} &= e^{iq\psi_{B\to Z}}e^{-\frac{q^2 a}{2l_{B\to Z}}},\\
\mathcal{D}_Z &= e^{iq\psi_Z}e^{-\frac{q^2 a}{2l_Z}},\\
\mathcal{D}_{Z\to B} &= e^{iq\psi_{Z\to B}}e^{-\frac{q^2 a}{2l_{Z\to B}}}.
\end{aligned} \tag{6}$$

We emphasize that the $M_{i,j}$ are compact resummations over all allowed distributions of domain walls for arbitrary bond-operators. To better illustrate the physical content of $M_{i,j}$, we may expand $M_{B,B}$ in powers of e^{-E}, which corresponds to an expansion in the number of domain walls. After the inverse Fourier transform we obtain, to the lowest order for Gaussian bonds:

$$M_{B,B} \sim \frac{e^{-\frac{l_B(\psi - n\psi_B)^2}{2na}}}{\sqrt{2\pi na/l_B}} + e^{-2E}\sum_{\nu=1}^{n-1}\nu e^{-(n-\nu)\epsilon}\frac{e^{-\frac{\left(\psi - \overline{\psi}(\nu)\right)^2}{2\sigma(\nu)}}}{\sqrt{2\pi\sigma(\nu)}} + \ldots \tag{7}$$

with

$$\overline{\psi}(\nu) \;=\; (n - \nu - 1)\psi_Z + (\nu - 1)\psi_B + \psi_{Z\to B} + \psi_{B\to Z}$$

and

$$\sigma(\nu) \;=\; a\left(\frac{n - \nu - 1}{l_Z} + \frac{\nu - 1}{l_B} + \frac{1}{l_{Z\to B}} + \frac{1}{l_{B\to Z}}\right).$$

This expansion is transparent: considering a system with n bonds, the first term corresponds to the case of no B-Z junction and the second term represents the series summation of the contributions with two junctions with

$\nu - 1$ bonds connecting B-state to B-state and $n - \nu - 1$ bonds Z-state to Z-state. $\psi_{Z\to B}$ and $\psi_{B\to Z}$ are the twist rate at interfaces (see Fig. 1). The matrix $M_{Z,B}$ also can be expanded in powers of e^{-E}:

$$M_{Z,B} \sim e^{-E}\sum_{\nu=0}^{n-1} e^{-(n-\nu)\epsilon}\frac{e^{-\frac{\left(\psi-\overline{\psi}(\nu)\right)^2}{2\sigma(\nu)}}}{\sqrt{2\pi\sigma(\nu)}} + \ldots \tag{8}$$

with

$$\overline{\psi}(\nu) \;=\; (n-\nu-1)\psi_Z + \nu\psi_B + \psi_{B\to Z}$$

and

$$\sigma(\nu) \;=\; a\left(\frac{n-\nu-1}{l_Z} + \frac{\nu}{l_B} + \frac{1}{l_{B\to Z}}\right).$$

The transition involves one domain wall and a number of basepairs in the B-state ranging from 0 to $n-1$, as the domain wall moves from the boundary fixed at B-state to the free boundary. Similarly, we obtain the matrix $M_{B,Z}$ as

$$M_{B,Z} \sim e^{-E}\sum_{\nu=0}^{n-1} e^{-\nu\epsilon}\frac{e^{-\frac{\left(\psi-\overline{\psi}(\nu)\right)^2}{2\sigma(\nu)}}}{\sqrt{2\pi\sigma(\nu)}} + \ldots \tag{9}$$

with

$$\overline{\psi}(\nu) \;=\; \nu\psi_Z + (n-\nu-1)\psi_B + \psi_{Z\to B}$$

and

$$\sigma(\nu) \;=\; a\left(\frac{\nu}{l_Z} + \frac{n-\nu-1}{l_B} + \frac{1}{l_{Z\to B}}\right).$$

Finally, we may also expand $M_{Z,Z}$:

$$M_{Z,Z} \sim \frac{e^{-\frac{l_Z(\psi-n\psi_Z)^2}{2na}}}{\sqrt{2\pi na/l_Z}}e^{-n\epsilon} + e^{-2E}\sum_{\nu=1}^{n-1}\nu e^{-\nu\epsilon}\frac{e^{-\frac{\left(\psi-\overline{\psi}(\nu)\right)^2}{2\sigma(\nu)}}}{\sqrt{2\pi\sigma(\nu)}} + \ldots \tag{10}$$

with

$$\overline{\psi}(\nu) \;=\; (\nu-1)\psi_Z + (n-\nu-1)\psi_B + \psi_{Z\to B} + \psi_{B\to Z}$$

and

$$\sigma(\nu) \;=\; a\left(\frac{\nu-1}{l_Z} + \frac{n-\nu-1}{l_B} + \frac{1}{l_{Z\to B}} + \frac{1}{l_{B\to Z}}\right).$$

The partition function for a strand with one end in the B-state and the other in the Z-state can be expressed with either of the off-diagonal terms, $M_{Z,B}$ or $M_{B,Z}e^{-\varepsilon}$, where the extra factor $e^{-\varepsilon}$ accounts for initiation of the chain from the monomer in Z-state. This shows that $\psi_{B\to Z} = \psi_{Z\to B}$ and $l_{B\to Z} = l_{Z\to B}$, which is expected. In the following, we keep both notations for a better legibility of the formulas. For an asymptotically large E and short sequences ($ne^{-E} \to 0$), these low-order terms in e^{-E} expansions (Eqs. 7–10) yield an accurate approximation. Physically, this approximation assumes that thermally activated extra domain walls are scarce.

The partition functions give direct access to torque statistics. Usually the torque is measured from the (small) angular deviation $\Delta\psi$ of a torsionally rigid device, of which the torsional rigidity is K. What can, for example, be measured, is breathing statistics. A number of turns is given and the statistics of the twist angle $\Delta\psi$ is recorded. Assuming a linear device, the torque exerted on the molecule is measured as $\tau = -K\Delta\psi$. The statistical weight W of the measured $\Delta\psi$ is

$$W \propto Z(\psi - \Delta\psi)e^{-K\Delta\psi^2/2}.$$

For a large value of K, the device measures the thermodynamically averaged torque and a torque distribution depending on K. A favorable value of K to detect single monomer events, with no or short handles, turns out to be at the level of the 20-pN nm/rad^2 (or 5-k_BT/rad^2) range (see below). Twist-angle fluctuations are moderate under those rigidities. For high-resolution instruments, K is lower by one order of magnitude, and thus the free thermal fluctuations of the device are accordingly larger and more states are sampled.

The precise nature of the B-Z interface is still debated. The number of basepairs belonging to the interface is found to be three or more in crystal structure (7). What seems well established is that there is at least one broken basepair in the interface. This explains the considerably high free-energy cost of E. We would also expect the interface to be torsionally soft. If several basepairs were broken, the interface should resemble L-DNA, which is ~5–10 times softer than the B-form. Above we modeled the interface by just one bond between two adjacent B-DNA and Z-DNA blocks. For better modeling of the interface, we introduce below a hyper-bond spanning over several basepairs. This problem is not directly amenable to a transfer matrix formulation because the length can increase by more than one basepair when adding an interface, but can be solved by the z-transform. Let us discuss the case where the interface is described by one hyper-bond spanning over n_J elementary bonds, and denote the corresponding bond operator kernel as $\mathcal{D}^{(n_J)}$. The recursion equations for the partition function now read as

$$\begin{aligned}\mathcal{Z}_B(n+1) \;&=\; \mathcal{D}_B\mathcal{Z}_B(n) + \theta[n-(n_J-1)] \\ &\quad\times\; \mathcal{D}^{(n_J)}_{Z\to B}\mathcal{Z}_Z(n-(n_J-1))e^{-E}, \\ \mathcal{Z}_Z(n+1) \;&=\; \mathcal{D}_Z\mathcal{Z}_Z(n)e^{-\epsilon} + \theta[n-(n_J-1)] \\ &\quad\times\; \mathcal{D}^{(n_J)}_{B\to Z}\mathcal{Z}_B(n-(n_J-1))e^{-\epsilon-E},\end{aligned} \tag{11}$$

with $\theta[x] = 1$, for $x \geq 0$ and $\theta[x] = 0$, for $x < 0$. The function $\theta[n - (n_J - 1)]$ ensures that the second term of the recursion relation contributes only if $n > n_J - 1$. (Equation 11 can be obtained starting out from an ordinary recursion on the number of steps m keeping track of the length n, which is the number of elementary bonds; after summing over the number of steps m, for a fixed length n, we end up with Eq. 11 keeping track on the length n only.) To solve this recursion we introduce the z-transform

$$Q(z) \;=\; \sum\nolimits_{n=0}^{\infty} Z(n)z^{-n},$$

which is the solution of the ordinary linear equations (in previous work we used a continuous representation for index n, which we recover for $n_J = 1$ in the expansion $q \sim 0$, $p = z - 1 \sim 0$, $e^{-E} << 1$, and $\varepsilon \sim 0$),

$$A_{i,j}(z)Q_j(z) \;=\; -zZ_i(n \;=\; 0):$$

$$\begin{aligned}&\begin{pmatrix}\mathcal{D}_B - z & \mathcal{D}^{(n_J)}_{Z\to B}z^{-(n_J-1)}e^{-E} \\ \mathcal{D}^{(n_J)}_{B\to Z}z^{-(n_J-1)}e^{-E-\epsilon} & \mathcal{D}_Ze^{-\epsilon} - z\end{pmatrix}\begin{pmatrix}Q_B \\ Q_Z\end{pmatrix} \\ &\quad= -z\begin{pmatrix}Z_B(0) \\ Z_Z(0)\end{pmatrix}.\end{aligned} \tag{12}$$

Solving for the characteristic functions Q_B, Q_Z, we obtain the z-transform of the $M_{i,j}$ defined as

$$Q_i(z) = M_{i,j}(z)Z_j(n = 0),$$

where the indices i,j run over {B,Z}. The expressions of $M_{i,j}(z)$ include the determinant of the matrix $\mathbf{A}$ in Eq. 12 and

$$(Det|\mathbf{A}|)^{-1} \equiv \prod_{p=1}^{2n_J} \frac{1}{z - z_p}, \tag{13}$$

with z_p as the roots of $Det|\mathbf{A}| = 0$. The z-transform is inverted according to

$$M(n) = \frac{1}{2\pi i}\oint M(z)z^{n-1}\mathrm{d}z,$$

where the contour encloses all singularities. Here, this amounts to the sum over the residues of $M(z)$. The poles are simple poles except for possible specific values of q. There are then $2n_J$ poles, which is technically similar to increasing the rank of the transfer matrix (in the case $n_J = 1$ above, we only had two poles $z_{1,2}$). We can directly write down the matrix elements $M_{i,j}$, such as for example

$$M_{B,B}^{(n_J)} = -\sum_{p=1}^{2n_J} \frac{1}{\prod_{\widehat{p}}(z_p - z_{\widehat{p}})}\left(\mathcal{D}_Z e^{-\epsilon} - z_p\right)z_p^n, \tag{14}$$

where the product runs over the set of indices $\widehat{p}$ including all indices except p. Other matrix elements can be obtained similarly. For the common case of high cooperativity ($ne^{-E} << 1$), we may expand the partition function $M_{B,B}$ in powers of e^{-2E}. Assuming Gaussian bonds, the expansion reads as

$$M_{B,B} \sim \frac{e^{-\frac{l_B(\psi - n\psi_B)^2}{2na}}}{\sqrt{2\pi na/l_B}} + e^{-2E}\sum_{\nu=1}^{n-2(n_J-1)-1} \nu e^{-(n-2(n_J-1)-\nu)\epsilon} \times \frac{e^{-\frac{\left(\psi - \overline{\psi}(\nu)\right)^2}{2\sigma(\nu)}}}{\sqrt{2\pi\sigma(\nu)}} + \ldots \tag{15}$$

with

$$\overline{\psi}(\nu) = (n - 2(n_J - 1) - 1 - \nu)\psi_Z + (\nu - 1)\psi_B + \psi_{Z\to B} + \psi_{B\to Z}$$

and

$$\sigma(\nu) = a\left(\frac{n - 2(n_J - 1) - 1 - \nu}{l_Z} + \frac{\nu - 1}{l_B} + \frac{n_J}{l_{Z\to B}} + \frac{n_J}{l_{B\to Z}}\right).$$

The expansion is similar to Eq. 7 except that the junction is represented by a hyper-bond spanning over n_J bonds. Below, we will mainly use the model with an elementary interfacial bond ($n_J = 1$) and stay within the more familiar transfer matrix representation. We use a twist shift different from the reported −0.4 turns (14) to match other observations. In the following section, we will explicitly consider the case of a Gaussian interfacial hyper-bond with $n_J = 2$ and standard twist shift −0.4 turns, and analyze it in both the torque and twist ensembles. We will show that in the torque-ensemble the junction effect can be (roughly) approximated by a single-bond junction with a smaller twist shift, at ~−0.1 turns. There is no satisfactory mapping of the junction on an elementary bond in the twist ensemble, as can also be seen from the series in Eq. 15.

To summarize, we are now equipped with a compact expression of the partition function in q-space, in Eq. 2. Next, we will use this expression directly as the partition function under imposed torque τ with $q = -i\tau$, in the so-called torque ensemble. We will also use its inverse Fourier transform, which applies to the case of imposed twist angle. In favorable cases (short sequence/high domain wall penalty), the (partial) partition function restricted to the lowest number of domain walls can be used as described in Eqs. 7–10 for Gaussian bonds.

RESULTS

We consider short DNA sequences of 10–60 basepairs (core sequence) that are switchable to Z-DNA inserted between two-canonical duplex DNA(B-DNA), called handles. Typically, the sequence switchable to Z-DNA is composed of $d(pGpC)_n$ repeats. The free energy cost for switching a basepair is $\varepsilon \approx 0.5\ k_BT$ (28) and the disruption of basepair stacking in the standard form costs the domain wall energy of $E = 9\ k_BT$ (zipper model) (14) or slightly smaller (10). The preferred twists of B-DNA and Z-DNA are $\psi_B = 2\pi/10$ and $\psi_Z = -2\pi/12$, respectively. We use these values below, unless stated otherwise. The twist modulus of B-DNA is known to be $l_B = 75$–100 nm, but the twist modulus of Z-DNA is not yet established. We assume that $l_Z \approx l_B$ for most of our calculations, and we further investigate the influence of the possible variation of torsional stiffness upon the B-Z transition for the case of $l_Z \neq l_B$. The torsional responses of the core sequence are investigated both in torque ensemble (under imposed torque) and in twist ensemble (under imposed twist), based on the model presented above.

Albeit it is not easy to control the torque directly in situ, several central features characterizing the B-Z transition can be captured by using the partition function $\mathcal{Z}_\tau$ in torque ensemble. In Fig. 2, the average twist $\langle\psi\rangle$ is represented with respect to the reference value $\psi_0 = n\psi_B$ for the core sequence of size n attached to the handles of total size n_H. The B-Z transition is depicted by the abrupt change in twist angle $\langle\psi\rangle$ (Fig. 2 *a*) and its sharp-peaked fluctuation $\langle(\psi - \langle\psi\rangle)^2\rangle$ at the critical torque (Fig. 2 *b*). The mean number of monomers in Z-states can be obtained by $\langle n_Z\rangle = -\frac{1}{\mathcal{Z}_\tau}\frac{\mathrm{d}\mathcal{Z}_\tau}{\mathrm{d}\epsilon}$, and the fraction of monomers in Z-state $\langle n_Z\rangle/n$ is shown in Fig. 2 *f*. The critical torque is larger (in magnitude) if more (i.e., stronger) constraints apply. A rough understanding of this behavior can be gained by considering the B-Z transition as a discontinuous transition between the all-B state and the all-Z state at the torque τ_c, where their Gibbs free energies intersect. This leads to the approximate critical torque $\tau_c \approx (\varepsilon + N_{DW}E/n)/(\psi_Z - \psi_B)$, below which Z-DNA is the preferred state.

For comparison, the $\langle\psi\rangle$-τ relations for two different handle sizes ($n_H = 300$ and 3000) are shown in Fig. 2, *a* and *c*, respectively. The response is linear before and after the transition and the slope in the linear regime is ~$(n + n_H)/l_t$. The domain wall energy of $E = 9\ k_BT$ is large enough to enforce a cooperative switching. As shown in Fig. 2 *g*, the average number of domain walls N_{DW} below τ_c are $N_{DW} = 0$, 1, and 2 for free-, mixed-, and fixed-boundary conditions, respectively. Fig. 2, *d* and *h*, demonstrates the effect of

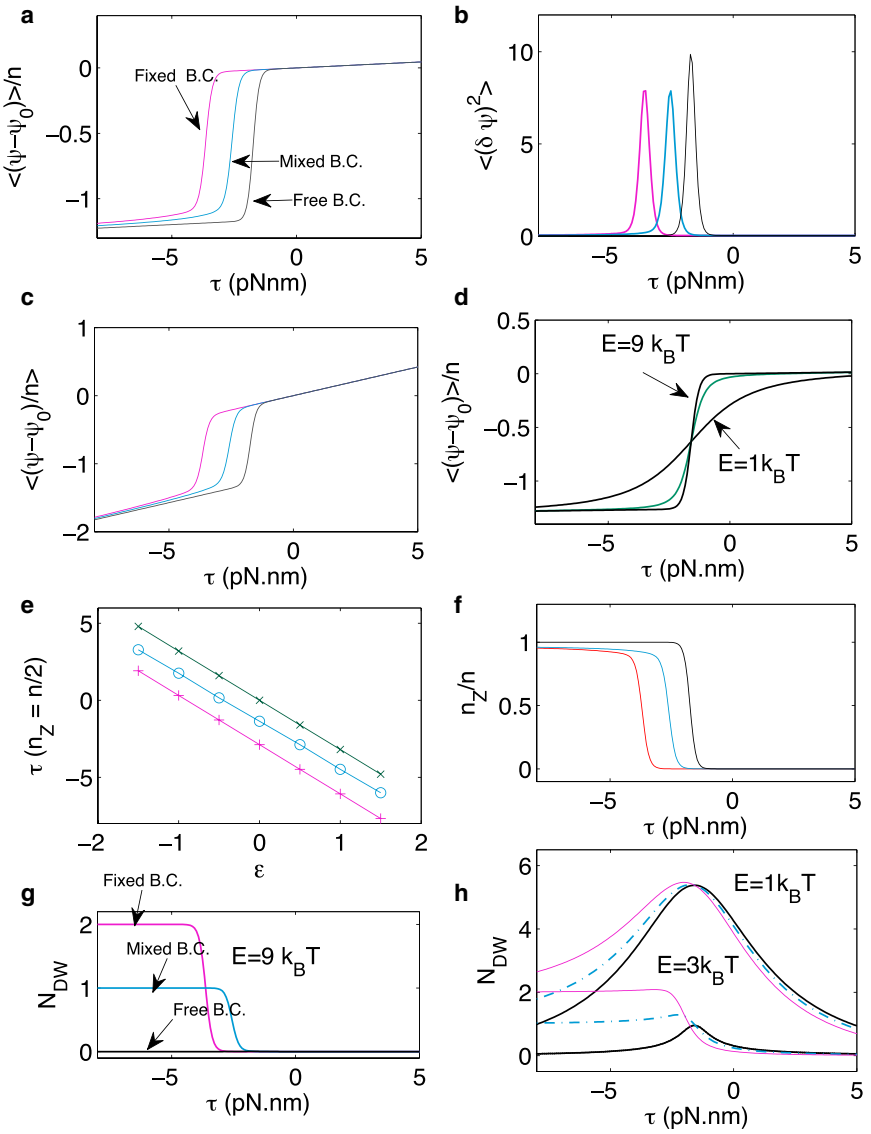

FIGURE 2 Torque-ensemble calculations for a core sequence of size $n = 30$ and $n_H = 300$. We use $E = 9\ k_BT$, $\epsilon = 0.5\ k_BT$, and $l_B = l_Z = l_J = 300a$, unless other values are specified. (*Magenta*, *blue*, and *black*) Fixed-, mixed-, and free-boundary condition for all panels, respectively, except for (*d*). (*a*) Average twist angle $\langle(\psi - \psi_0)/n\rangle$ and (*b*) its variance. (*c*) $\langle\psi\rangle$-τ relations with a handle of $n_H = 3000$ and (*d*) with different domain wall energies $E = 1$, 3, and 9 k_BT under free-boundary condition. (*e*) Transition torque ($n_Z = n/2$) as a function of ϵ. (*f*) The fraction of monomers in Z-state n_Z/n. (*g*) The number of domain walls N_{DW} with $E = 0\ k_BT$ and (*h*) with smaller domain wall energies ($E = 1$, 3 k_BT). To see this figure in color, go online.

domain wall energy E. The transition is less cooperative for small E, and $\langle\psi\rangle$ and N_{DW} vary continuously across the transition torque τ_c. The mean number of domain walls N_{DW} has a maximum for sufficiently small $E \sim 1\ k_BT$. Fig. 2 *e* summarizes the shift of the midpoint torque τ_c, where the B/Z states exist with an equal probability, as a function of ϵ. Here (Fig. 2) we used the interface twist $\psi_J = -0.1 \times 2\pi$ over a junction with size of unity. The choice of this value can be justified through the comparison with more involved calculation using the hyper-bond description, which takes into account more accurately the actual twist of $\psi_J = -0.4 \times 2\pi$ over the interface of $n_J > 1$.

Fig. 3 shows the average twist angle and the variance as calculated from the hyper-bond description (*black solid line*) with ψ_J and a single bond with an adjusted twist angle ψ_J'. With $\psi_J' = -0.12 \times 2\pi$, the single bond calculation fits best the hyper-bond model calculation with the actual twist $\psi_J = -0.4 \times 2\pi$. Below the twist angle shift at junction ψ_J is assumed to be $\psi_J = -0.1 \times 2\pi$ if the junction is treated as a single bond.

Most single-molecule experiments are carried out by controlling the twist angle. For short highly cooperative cores, we can assess the torque, n_Z, and N_{DW} at a given twist angle ψ using the partition functions given by Eqs. 7 and 8 or equivalently by the more general equations, such as Eqs. 4 and 5, for mixed-/fixed-boundary conditions. Below we discuss the twist(δLk)-torque(τ) relation when the extra linking number δLk is controlled, which we refer to as twist ensemble. In Fig. 4, the torque, n_Z, and N_{DW} are computed for a core sequence of length $n = 10$ flanked by handles of various sizes ($n_H = 50$, 100, 300, and 500) under the fixed-boundary conditions. The B-Z transition region is depicted as a pseudo plateau (τ_c) between two linear response regimes. Following the derivation in previous studies (3), the torque at the onset of the transition is

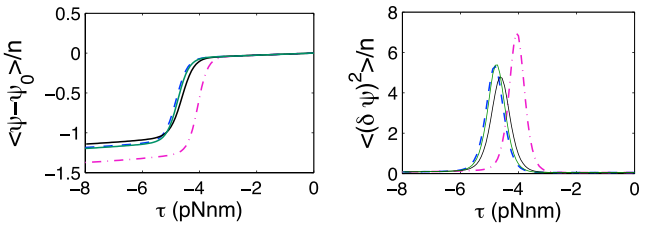

FIGURE 3 Torque ensemble; fixed-boundary conditions. Comparison of the single-bond and the hyper-bond descriptions. The interface taking $\psi_J = -0.4 \times 2\pi$ is treated by two methods: (*left*) hyper-bond of length $n_J = 2$, and (*right*) a single-bond with an adjusted ψ_J'. (*Black solid line*) Average twist angle and (*right*) variance calculated from the hyper-bond description; (*blue*, *green*, and *magenta*) for the single-bond junction, the cases with $\psi_J' = -0.1 \times 2\pi$, $-0.12 \times 2\pi$, and $-0.4 \times 2\pi$ are represented, respectively. The value $\psi_J' = -0.12 \times 2\pi$ fits best to the hyper-bond description with $\psi_J = -0.4 \times 2\pi$. Here we use $E = 0.5\ k_BT$, $E = 9\ k_BT$, and $l_B = l_Z = l_J = 300a$. To see this figure in color, go online.

$$\tau_{tr} \approx \epsilon/(\psi_Z - \psi_B) - \sqrt{2N_{DW}E\frac{l_t}{S}}$$

and depends on both ϵ and the domain wall energy E. The first term corresponds to the plateau value of the critical torque τ_c and the second term corresponds to the difference between the plateau torque and the minimum. Provided that $l_B = l_Z = l_J = l_t$, the effective stiffness of the chain is $\sim l_t/(n + n_H)$ in the linear response regimes. With the shortest handle size ($n_H = 50$), the response of the core sequence appears to be undulating. Each peak is related to the event of switching one monomer, which results in the torque undulation. For a short core sequence with short or no handles, the partition function is dominated by a single state with well-defined n_Z, which increases as negative

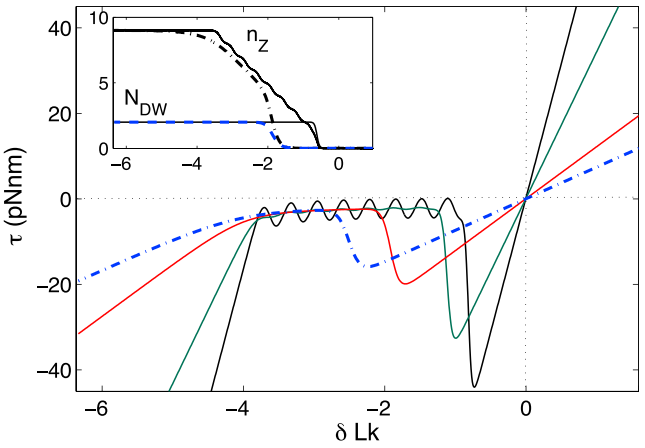

FIGURE 4 Twist ensemble; fixed-boundary conditions. Torque is computed as a function of the controlled twist δLk. The core length is $n = 10$ and the handle size takes values from $n_H = 50$, 100, 300, and 500 (shown as *black*, *green*, *red*, and *blue lines*). (*Inset*) Number of Z-state monomers n_Z and the number of the domain walls N_{DW} for $n_H = 50$ (*solid line*) and 500 (*dashed line*). We use $E = 0.5\ k_BT$, $E = 9\ k_BT$, and $l_B = l_Z = l_J = 300a$. To see this figure in color, go online.

turns are added (see the *inset* of Fig. 4). In each of these subregimes, the torque vanishes for a particular value of the twist. The torque hence undulates around the quasi-plateau with maxima of zero torque. During the B-Z transition, the torsional stress relaxes by switching the monomer state. The transition regime spans over $\sim(n-1)(\psi_B - \psi_Z)/(2\pi)$ until all the basepairs are switched to Z-state. There is an apparent reduction in the length of the actual plateau as the handle size grows. It is because n_Z increases somewhat abruptly at the start of the transition reflecting the energy penalty for nucleation of Z-domain. The plateau corresponds to the regime where n_Z increases linearly with δLk. The end of the B-Z transition, corresponding to the saturation of n_Z in the inset of Fig. 4, is shifted to more negative twist. With large handles, torque undulations responding to the monomer switching are washed out by large thermal fluctuations.

In order to make better comparison with experimental results (11,12), we consider system sizes more common in magnetic tweezers experiments. Fig. 5 shows a series of torque-twist relations computed for a 10–60-bp-long core sequence with a ~5000-bp-long handles as considered in Oberstrass et al. (11,12). The computed results recover some of the existing results—boundary effects and the extent of the transition regime agree with the results of Oberstrass et al. (11,12) and Lebel et al. (29) (see, for example, Figs. 2 and 3 in Oberstrass et al. (12)). Under free-boundary conditions, a torque overshoot is seen when the B-Z boundary disappears, as shown in the middle panel. Doubling free energy ϵ leads to a larger (in magnitude) critical torque, which we expect to see from the core sequence of $(TG)_n$ repeats (28).

We compute torque distributions under the given twist angle ψ^*, which is shared by the molecule taking ψ_s and the (rigid) device taking $\Delta\psi = \psi^* - \psi_s$. The twist of the free device is fluctuating with variance of k_BT/K, where K is the torsional spring constant of the device. In Fig. 6, we plot the torque distribution that reflects breathing, under the fixed-boundary condition. For a molecule under twist angle ψ_s, the torque measured by the device is $\tau =$

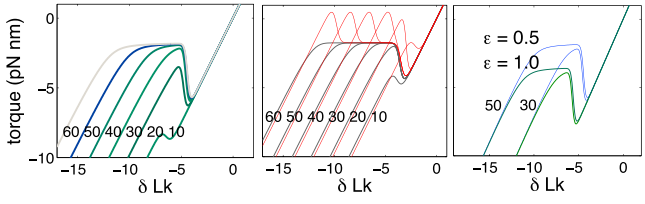

FIGURE 5 Twist ensemble. Twist(δLk)-torque(τ) relations for various core sizes $n = 10$, 20, 30, 40, 50, and 60. The handle size is fixed as $n_H = 5000$ and we use $E = 9\ k_BT$ and $l_B = l_Z = l_J = 300a$. (*Curves*, *left panel*) Fixed-boundary conditions; (*middle panel*) free- (*red*) and mixed- (*black*) boundary conditions. (*Right panel*) We compare curves obtained for different values of ϵ (0.5 k_BT and 1.0 k_BT) and for different core sizes ($n = 30$ and 50) under fixed-boundary conditions. To see this figure in color, go online.

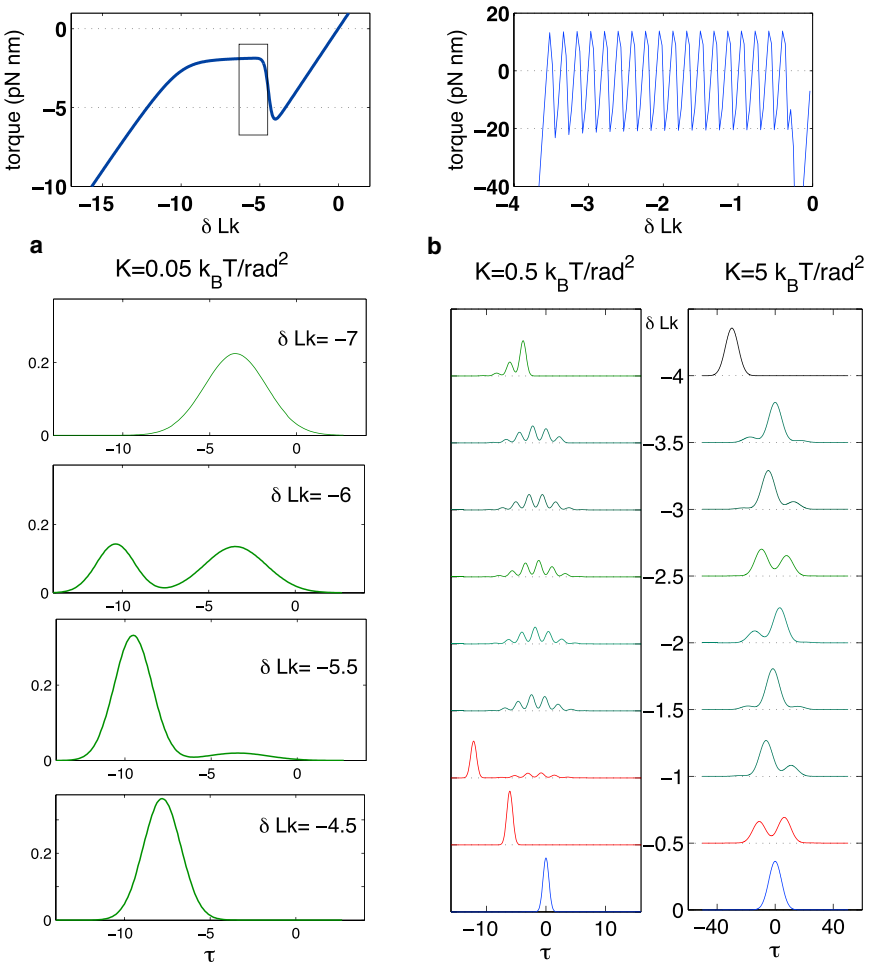

FIGURE 6 Twist ensemble. δLk-τ relations (*top*) and torque histograms (*bottom*) at imposed twists $\delta Lk = (\psi^* - n\psi_B)/2\pi$ are computed for chains with (*a*) $n = 50$ and handle size $n_H = 5000$ (fixed boundary) and with (*b*) $n = 20$ without any handle. The spring constant of the harmonic potential is $K = 0.05\ k_BT/\text{rad}^2$ (*a*) and $K = 0.5\ k_BT/\text{rad}^2$ (*b*, *left*) and $5\ k_BT/\text{rad}^2$ (*b*, *right*). The imposed twist δLk ranges from 0 to −4 as indicated between two panels of (*b*). We use $E = 9\ k_BT$, $\varepsilon = 0.5\ k_BT$, $l_B = l_Z = l_J = 300a$, and $\psi_J = -0.1 \times 2\pi$. The coexistence of multiple states with different n_Z values is depicted by multiple overlapping Gaussian peaks in the transition regime. The histograms are normalized so that the area below is to be unity. To see this figure in color, go online.

$-K\Delta\psi$. Fig. 6 *a* shows the torque histograms for the imposed twist $\delta Lk = (\psi^* - n\psi_B)/(2\pi)$ computed for a chain of $n = 50$ and handle size of $n_H = 5000$. The molecular spring constant is set to $K = 0.05\ k_BT/\text{rad}^2$, which is comparable to the experimental value in Lebel et al. (29). The width of the measured torque distribution is small before the B-Z transition and is much bigger in the transition regime (~$k_BT \approx 4$ pN/nm), as seen from Fig. 5 of Lebel et al. (29). The calculated distribution is bimodal at the transition regime between $\delta Lk = -5$ and -6. The broad distribution implies that many metastable states contribute. We also calculate the torque distribution for the bare core sequence to capture the microscopic event of monomer state switching. The left and right panels of Fig. 6 *b* show the distribution obtained with $K = 0.5\ k_BT/\text{rad}^2$ (*left panel*) and $5\ k_BT/\text{rad}^2$ (*right panel*), respectively. From bottom to top, the torque histograms are arranged with decreasing $\delta Lk = (\psi^* - n\psi_B)/(2\pi)$ as indicated between two panels. With $\delta Lk = 0$, all monomers are in B-state showing a single peak at $\tau = 0$. The peak position moves from zero to negative τ with decreasing δLk. At the start of the transition ($\delta Lk^* = -0.95$), smaller peaks (attributed to the states with $n_Z = 2,3$) appear in the left panel. At intermediate δLk, the distribution is a multiple Gaussian, where each peak represents a different n_Z-state with comparable statistical weights, which are reversibly switchable. However, the torque populations from different states are separated by $< k_BT$. In experiments, these separations of single events are expected to be washed away due to the thermal fluctuation of the handles. For sufficiently small δLk, the distribution is single Gaussian again, which can be attributed to all Z-state. The histograms obtained with a larger value of $K = 5\ k_BT/\text{rad}^2$ (*right panel*) exhibit only one or two peaks during the B-Z transition. The typical form is double Gaussian during the B-Z transition and two switchable n_Z states contribute. The separation between the peaks is ~5 k_BT.

Fig. 7 *a* demonstrates the torque response with alternative values of $l_Z \neq l_B$. For sufficiently negative torsion, all core basepairs switch to Z-DNA. Then, after the B-Z transition, the expected slope in linear regime is $\sim 1/(n_H/l_B + n/l_Z)$. For $l_Z \geq l_B/2$, the torque response shows little deviation from the relation with $l_Z = l_B$. Assuming the same geometry as the experiment under consideration where $n_H/n = 100$, a noticeable change in the slope such as 10% as reported in the experiment with fixed-boundary condition (Fig. 1 of

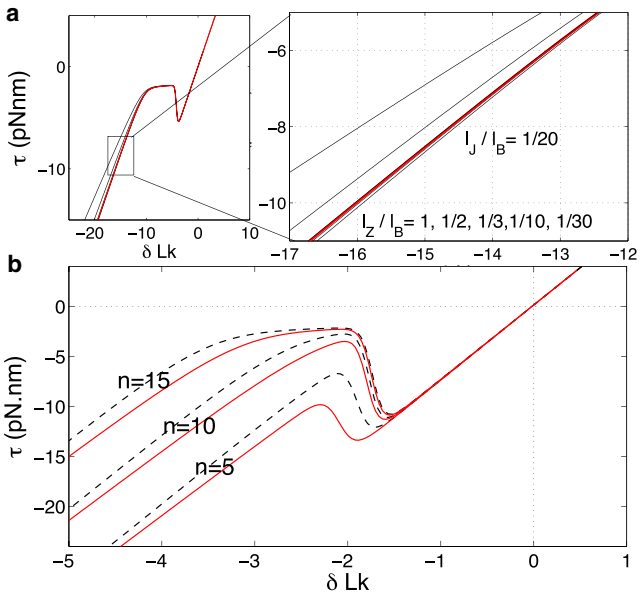

FIGURE 7 Twist ensemble; fixed boundary. (*a*) δLk-τ relations of a chain ($n = 50$ and $n_H = 5000$) for various values of torsional modulus of Z-DNA, l_Z, with single-bond B-Z interfaces ($l_J = l_B$, $\psi_J = -0.1 \times 2\pi$). (*Top* to *bottom*) Moduli of Z-DNA are l_Z/l_B = 1/30, 1/10, 1/3, 1/2, and 1. (*Red*) Calculation for a chain with soft hyper-bond interfaces ($n_J = 2$, $\psi_J = -0.4 \times 2\pi$ and modulus $l_J = l_B/20$). Here we assume $l_Z = l_B$. (*b*) (*Solid lines*) Hyper-bond calculation for short cores of sizes n = 5, 10, and 15 with n_H = 1000. (*Dashed lines*) For each case, the single-bond interface ($l_J = l_Z = l_B$) results are shown for comparison. We use $\epsilon = 0.5\ k_BT$, $E = 9\ k_BT$, and $l_B = 300a$. To see this figure in color, go online.

Oberstrass et al. (12)) is observed if the twist persistence length of Z-DNA is as small as $l_Z = l_B/3$. Alternatively, some additional softening can be expected if l_J is very small. Using the hyper-bond description, we explicitly take into account the B-Z junction in the calculation of the torsional response. A slope change of 10% due to the soft junction, even with an equally large modulus of Z-DNA $l_Z \approx l_B$, corresponds to a junction modulus of $l_J = l_B/20$ (shown as *red line* in Fig. 7 *a*). This gives a junction modulus $l_J \approx 5$ nm. We also note that the modulus of L-DNA falls into this range (~10 nm) (5). This result suggests that the soft modulus after full conversion to Z-DNA12 is not only because of the Z-DNA modulus but also due to the soft modulus of the B-Z junction of finite size. The use of short handles would enhance the slope deviation due to the modulus variation. To investigate the influence of junction size, we consider chains including a short switchable sequence n under fixed-boundary conditions (see Fig. 7 *b*). A clear signature of junction size can be seen when the two necessary junctions interact upon switching to Z-DNA. If the junction spans over n_J bonds, the minimal section occupied by an interface covers at least $2n_J + 1$ monomers. Energy cost for switching such a short core is comparable to the junction energy penalty while only 0.8 turns are taken. Thus the transition is delayed for chains with a short core. The hyper-bond model calculation shows that the B-Z transition is shifted to more negative torsional stress than the estimate from the single-bond interface model.

We examine the effect of junction twist angle. The B-Z transition depends qualitatively on the size of the junction angle ψ_J, as can be seen from δLk-τ relations under fixed- and free-boundary conditions. Fig. 8 shows n_Z, n_{DW}, and τ for various values of ψ_J within the single-bond junction description. For a large junction twist angle ($\psi_J = -0.4 \times 2\pi$), a torque overshoot is seen at the beginning of the B-Z transition. This overshoot is enhanced for the fixed boundary (see *inset* of Fig. 8 *a*) and can be seen only with short handles (comparable to the core size). It also resembles the kinetic effects with long handles, as reported in Oberstrass et al. (11). Within the single-bond junction model, a torque overshoot at the onset of transition does not exist if $|\psi_J| \leq 0.2 \times 2\pi$ for all handle sizes.

Under free boundary conditions, a torque overshoot is always seen for the values of junction twist ψ_J we tested, when the B-Z boundary disappears ($N_{DW} = 0$) and all core sequences turn to Z-state. If $\delta Lk << 0$, a large junction twist $\psi_J = -0.4 \times 2\pi$ causes undulations in torque beyond the transition regime. Some part of the core sequence turns back to B-state by trading the Z-states with junctions. The amplitude of such undulation is large for the chains with short handles and remains to some extent for an intermediate handle size of $n_H = 500$. For even larger handles (n_H = 1000), the unexpected curvature is still seen.

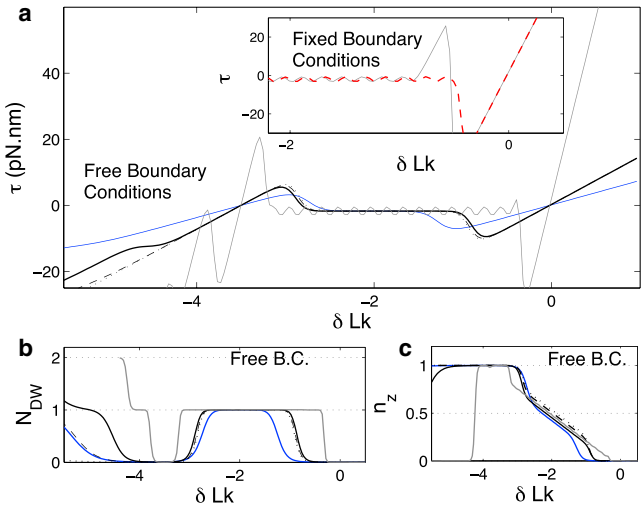

FIGURE 8 Twist ensemble; single-bond junction description. (*a*) The effect of junction twist angle and handle length on δLk-τ relations for a core of $n = 20$ under free-boundary conditions. (*Solid lines*) For $\psi_J = -0.4 \times 2\pi$, the data with various handle lengths $n_H = 50$ (*gray*), 500 (*black*), and 1000 (*blue*). (*Dashed lines*) Data for $\psi_J = -0.1 \times 2\pi$ and (*dotted lines*) data for $\psi_J = -0.2 \times 2\pi$ with $n_H = 500$. (*b* and *c*) N_{DW} and n_Z as a function of δLk. (*Inset*, *a*) Torque response under fixed-boundary conditions where $\psi_J = -0.4 \times 2\pi$ and the lengths of handle are $n_H = 50$ (*gray solid*) and $n_H = 500$ (*red dashed*). We use $\epsilon = 0.5\ k_BT$, $E = 9\ k_BT$, and $l_B = l_Z = l_J = 300a$. To see this figure in color, go online.

DISCUSSION

We propose a model to describe the partition function of a single DNA molecule undergoing the B-Z transition by using the bond operator (30) representation for annealed copolymers (31). The theory takes advantage of the simple (multiplicative) form of the bond operators in Fourier space with the momentum q being conjugate to the twist angle ψ. In the simplest case considered, where we treat B-Z interfaces as single bonds, the theory reduces to a transfer matrix problem for the Fourier-transformed partition function. We exploit the Fourier-transformed partition function in two ways, either by injecting the imaginary momentum $q = -i\tau$, which yields the partition function under imposed torque τ (torque ensemble), or by inverting it to yield the partition function under imposed twist angle (twist ensemble). For Gaussian bonds (linear elasticity), the main ingredients of the bond operators are the preferred twist angle per bond and the bond twist-rigidity, which are a priori different for the B-form, the Z-form, and the B-Z interface. Besides, there are two energetic parameters, the free energy difference ϵ between a basepair in the Z-form and the B-form and the free energy penalty E for a B-Z interface. Our model does accommodate more complex bond operators, beyond Gaussian (25–27).

Under an imposed torque we discuss the transition as a function of the parameters ϵ (Fig. 2). Highly cooperative transitions are observed for $E = 9\ k_BT$ where the equation of state (average twist versus torque) shows a steplike variation. The transition is shifting to larger torque (in magnitude) when more constraining boundary conditions are imposed (free → mixed → fixed) for the short core sequences. The shift is substantial when the (minimum) number of B-Z interfaces involved in the transition increases (from 0 to 2). NMR experiments performed on short DNA oligomers (13) report high B-to-Z conversion rate at low Z-DNA binding protein concentrations, which also supports the predicted easy conversion under free-boundary conditions (Fig. 2).

Under an imposed twist, we discuss the transition under various boundary conditions (free, mixed, fixed). Without handles, the transition region is manifested as a clean quasi-plateau of torque albeit with small wiggles revealing single basepair switching events (the latter may be washed out by the device). In the presence of handles, as is the case for most experiments, the step is smoothened but the span of the plateau is (markedly) shorter (Fig. 4), as reported in experiments. The cases where the B-Z transition couples with the B-L transition of the handles are more involved. If the handles remain stable, the rigidity (slope) after the conversion of the core sequence to the Z-form should reveal the torsional stiffness of the Z-form plus junctions. An extended discussion of the breathing (Fig. 6) and device twist-angle distribution (or torque distribution) under an imposed number of turns shows single switching events (two close states populated) or more maxima corresponding to a larger collection of populated states, depending on the device rigidity and the length of handles. Within our model, we also analyzed the influence of the twist shift through the B-Z interface on the transition (Fig. 8). Larger values of the twist shift within a single-bond (like -0.4 turns) lead to unexpected curvature after the conversion plateau. (Such effects have not been reported in experiments.) For shorter handles ($n_H = 50, 500$), there are oscillations. In the single-bond junction model, moderate shifts (like -0.1 turns) are more consistent with experimental observations.

We also present a model with an interfacial hyper-bond extending over n_J elementary bonds (Fig. 7). This picture is compatible with the known crystal structure (7,18) suggesting that there is at least one extruded basepair in the interface. We analyzed the model in both torque and twist spaces. There is no exact mapping between the hyper-bond model and the single-bond model. Nevertheless, an interfacial hyper-bond with $n_J = 2$ and $\psi_J = -0.4 \times 2\pi$ behaves closer to an elementary interfacial bond, with $n_J = 1$ and a weaker twist-shift around -0.1 turns in a torque ensemble. We postpone a detailed analysis of the hyper-bond model to future work. Indeed, although we believe that a proper description of the junctions goes beyond linear elasticity, the progress critically depends on chemically realistic simulations or dedicated experiments. A high-resolution torque measurement experiment (29) performed on a short switchable sequence with fixed boundary conditions may assess the junction's elasticity and length via the (non-Gaussian) hyper-bond model. This should help understanding the junction structure in situ, which may not correspond to the one known previously from the crystal structure of Z-DNA (7,18).

Our model can be adapted to other systems with annealed degrees of freedom either torsional or flexural, for example, or for actin filaments with twist disorder (32) and filaments with annealed bending stiffness (33) or annealed curvature (34–36).

ACKNOWLEDGMENTS

N.-K.L. acknowledges financial support from the Korean Research Foundation via grants No. 2012R1A1A3013044 and No. 2014R1A1A2055681. N.-K.L. and A.J. acknowledge support from the Star Exchange Program (grant No. NRF-2012K1A3A1A21030441). This work is also supported by Korean Research Foundation grant No. 2012R1A1A2021736 (to S.-C.H.).

REFERENCES

1. Salerno, D., A. Tempestini, …, F. Mantegazza. 2012. Single-molecule study of the DNA denaturation phase transition in the force-torsion space. *Phys. Rev. Lett.* 109:118303.
2. Mosconi, F., J.-F. Allemand, …, V. Croquette. 2009. Measurement of the torque on a single stretched and twisted DNA using magnetic tweezers. *Phys. Rev. Lett.* 102:078301.
3. Son, A., A.-Y. Kwon, …, N. K. Lee. 2014. Underwound DNA under tension: L-DNA vs. plectoneme. *EuroPhys Lett.* 105:48002.

4. Marko, J. F., and S. Neukirch. 2013. Global force-torque phase diagram for the DNA double helix: structural transitions, triple points, and collapsed plectonemes. *Phys. Rev. E Stat. Nonlin. Soft Matter Phys.* 88:062722.
5. Sheinin, M. Y., S. Forth, …, M. D. Wang. 2011. Underwound DNA under tension: structure, elasticity, and sequence-dependent behaviors. *Phys. Rev. Lett.* 107:108102.
6. Rich, A., A. Nordheim, and A. H. Wang. 1984. The chemistry and biology of left-handed Z-DNA. *Annu. Rev. Biochem.* 53:791–846.
7. Fuertes, M., V. Cepeda, …, J. Pérez. 2006. Molecular mechanisms for the B-Z transition in the example of poly[d(G-C)•d(G-C)] polymers. A critical review. *Chem. Rev.* 106:2045–2064.
8. Herbert, A., and A. Rich. 1996. The biology of left-handed Z-DNA. *J. Biol. Chem.* 271:11595–11598.
9. Lim, W. 2007. Solitary excitations in B-Z DNA transition: a theoretical and numerical study. *Phys. Rev. E Stat. Nonlin. Soft Matter Phys.* 75:031918.
10. Lee, M., S. H. Kim, and S.-C. Hong. 2010. Minute negative superhelicity is sufficient to induce the B-Z transition in the presence of low tension. *Proc. Natl. Acad. Sci. USA.* 107:4985–4990.
11. Oberstrass, F. C., L. E. Fernandes, and Z. Bryant. 2012. Torque measurements reveal sequence-specific cooperative transitions in supercoiled DNA. *Proc. Natl. Acad. Sci. USA.* 109:6106–6111.
12. Oberstrass, F. C., L. E. Fernandes, …, Z. Bryant. 2013. Torque spectroscopy of DNA: base-pair stability, boundary effects, backbending, and breathing dynamics. *Phys. Rev. Lett.* 110:178103.
13. Kang, Y.-M., J. Bang, …, J.-H. Lee. 2009. NMR spectroscopic elucidation of the B-Z transition of a DNA double helix induced by the Zα domain of human ADAR1. *J. Am. Chem. Soc.* 131:11485–11491.
14. Peck, L. J., and J. C. Wang. 1983. Energetics of B-to-Z transition in DNA. *Proc. Natl. Acad. Sci. USA.* 80:6206–6210.
15. Pohl, F. M., and T. M. Jovin. 1972. Salt-induced co-operative conformational change of a synthetic DNA: equilibrium and kinetic studies with poly (dG-dC). *J. Mol. Biol.* 67:375–396.
16. Schwartz, T., J. Behlke, …, A. Rich. 2001. Structure of the DLM-1-Z-DNA complex reveals a conserved family of Z-DNA-binding proteins. *Nat. Struct. Biol.* 8:761–765.
17. Thomas, T. J., and T. Thomas. 1994. Polyamine-induced Z-DNA conformation in plasmids containing (dA-dC)n•(dG-dT)*n* inserts and increased binding of lupus autoantibodies to the Z-DNA form of plasmids. *Biochem. J.* 298:485–491.
18. Ha, S. C., K. Lowenhaupt, …, K. K. Kim. 2005. Crystal structure of a junction between B-DNA and Z-DNA reveals two extruded bases. *Nature.* 437:1183–1186.
19. Wang, G., and K. M. Vasquez. 2007. Z-DNA, an active element in the genome. *Front. Biosci.* 12:4424–4438.
20. Vologodskii, A. V., and M. D. Frank-Kamenetskii. 1984. Left-handed Z form in superhelical DNA: a theoretical study. *J. Biomol. Struct. Dyn.* 1:1325–1333.
21. Frank-Kamenetskii, M. D., and A. V. Vologodskii. 1984. Thermodynamics of the B-Z transition in superhelical DNA. *Nature.* 307:481–482.
22. Zhabinskaya, D., and C. J. Benham. 2011. Theoretical analysis of the stress induced B-Z transition in superhelical DNA. *PLOS Comput. Biol.* 7:e1001051.
23. Bryant, Z., M. D. Stone, …, C. Bustamante. 2003. Structural transitions and elasticity from torque measurements on DNA. *Nature.* 424:338–341.
24. Lipfert, J., J. W. J. Kerssemakers, …, N. H. Dekker. 2010. Magnetic torque tweezers: measuring torsional stiffness in DNA and RecA-DNA filaments. *Nat. Methods.* 7:977–980.
25. Weysser, F., O. Benzerara, …, I. Kulić. 2015. Topological energy storage of work generated by nanomotors. *Soft Matter.* 11:732–740.
26. Marko, J. F. 2009. Linking topology of tethered polymer rings with applications to chromosome segregation and estimation of the knotting length. *Phys. Rev. E Stat. Nonlin. Soft Matter Phys.* 79:051905.
27. Walter, J. C., G. T. Barkema, and E. Carlon. 2011. The equilibrium winding angle of a polymer around a bar. *J. Stat. Mech.* P10020.
28. Ho, P. S. 1994. The non-B-DNA structure of d(CA/TG)n does not differ from that of Z-DNA. *Proc. Natl. Acad. Sci. USA.* 91:9549–9553.
29. Lebel, P., A. Basu, …, Z. Bryant. 2014. Gold rotor bead tracking for high-speed measurements of DNA twist, torque and extension. *Nat. Methods.* 11:456–462.
30. Grosberg, A. Y., and A. R. Khokhlov. 1994. Statistical Physics of Macromolecules. American Institute of Physics, New York.
31. Grosberg, A. Y. 1984. Collapse and intramolecular phase separation in the polymer in which each link may be in two states. *Biofizika.* 29:569.
32. Egelman, E. H. 2001. Actin allostery again? *Nat. Struct. Biol.* 8:735–736.
33. Fierling, J., H. Mohrbach, …, A. Johner. 2014. Biofilaments as annealed semi-flexible copolymers. *EuroPhys Lett.* 106:58006.
34. Mohrbach, H., A. Johner, and I. M. Kulić. 2010. Tubulin bistability and polymorphic dynamics of microtubules. *Phys. Rev. Lett.* 105:268102.
35. Nam, G., N. Lee, …, I. Kulić. 2012. Helices at interfaces. *EuroPhys Lett.* 100:28001.
36. Fierling, J., M. M. Müller, …, I. K. Kulić. 2014. Crunching biofilament rings. *EuroPhys Lett.* 107:68002.